Scientific Research Publishing

International Journal of Geosciences, 2024, 15, 162-179
https://www.scirp.org/journal/ijg
ISSN Online: 2156-8367
ISSN Print: 2156-8359

# Petrophysical Evaluation of Cape Three Points Reservoirs

**Striggner Bedu-Addo[1*], Sylvester Kojo Danuor[1], Larry Pax Chegbeleh[2]**

[1]Department of Physics, Kwame Nkrumah University of Science and Technology, Kumasi, Ghana
[2]Department of Earth Science, University of Ghana, Accra, Ghana
Email: *striggnerbeduaddo@gmail.com

**How to cite this paper:** Bedu-Addo, S., Danuor, S.K. and Chegbeleh, L.P. (2024) Petrophysical Evaluation of Cape Three Points Reservoirs. *International Journal of Geosciences*, **15**, 162-179.
https://doi.org/10.4236/ijg.2024.152011

**Received:** December 29, 2023
**Accepted:** February 26, 2024
**Published:** February 29, 2024



## Abstract

The findings of a study to ascertain and assess the petrophysical characteristics of Cape Three Points reservoirs in the Western basin with a view to describe the reservoir quantitatively using Well Logs, Petrel and Techlog. The investigated characteristics, which were all deduced from geophysical wire-line logs, include lithology, porosity, permeability, fluid saturation, and net to gross thickness. To characterise the reservoir on the field, a suite of wire-line logs including gamma ray, resistivity, spontaneous potential, and density logs for three wells (WELL_1X, WELL_2X, and WELL_3X) from the Tano Cape Three Point basin were studied. The analyses that were done included lithology delineation, reservoir identification, and petrophysical parameter determination for the identified reservoirs. The tops and bases of the three wells analysed were marked at a depth of 1203.06 - 2015.64 m, 3863.03 - 4253.85 m and 2497.38 - 2560.32 m respectively. There were no hydrocarbons in the reservoirs from the studies. The petrophysical parameters computed for each reservoir provided porosities of 13%, 3% and 11% respectively. The water saturation also determined for these three wells (WELL_1X, WELL_2X and WELL_3X) were 94%, 95% and 89% respectively. These results together with the behaviour of the density and neutron logs suggested that these wells are wildcat wells.

## Keywords

Petrophysical, Cape Three Points, Reservoirs

## 1. Introduction

Hydrocarbon bearing reservoir, source rocks, cap rocks, and aquifers are recognized and assessed using rock properties and their relationships. Petrophysics is the study of the physical and chemical properties of rocks and their contained fluids [1]. The oil industry places great importance on these petrophysical properties—porosity, permeability, fluid saturation, capillarity, etc.—because they constitute a set of fundamental engineering parameters and continue to be the fundamental means of obtaining trustworthy data that allows reservoir rock to be quantitatively described in order to assess the economic viability of hydrocarbon-bearing reservoirs [2]. However, a reservoir is a subsurface layer or series of porous rock layers that hold hydrocarbons; these layers are often carbonate or sandstone rock, depending on their geological origin [3]. Sadly, it is not possible to directly measure these petrophysical properties; instead, one must infer them from measurements of other reservoir rock parameters, such as the rock's resistivity, bulk density, interval transit time, spontaneous potential, natural radioactivity, and hydrogen content [4]. These parameters however are measured using well logs which are categorized into three groups: electrical, nuclear and acoustic. Electric logs include induction logs, and normal and lateral resistivity logs. Nuclear logging methods are utilized to measure bulk density and neutron responses, and natural gamma ray energies. Acoustic logs are used to estimate porosity and lithology as well as to tie into seismic data). Acoustic logs may also reveal much about the mechanical properties and texture of the formation [5]. The assessment of the probable productivity of permeable and porous strata encountered by a drill is the goal of well log interpretation. In conjunction with core analysis, a well-run logging programme can provide information for mapping subsurface structures, define the lithology, locate productive zones and precisely characterise their depth and thickness, differentiate between oil and gas, and enable a reliable quantitative and qualitative interpretation of reservoir properties like porosity, permeability, fluid saturation, and capillarity, etc. (Schlumberger, 1989). This paper seeks to analyse and evaluate the hydrocarbon potential in the CTP reservoirs using three wells (WELL_1X, WELL_2X and WELL_3X) and modern-day industrial wireline well logs to estimate the petrophysical properties of the reservoir.

## 2. Study Area

Regionally, the Tano Cape Three Points (CTP) block is located on the continental shelf, offshore southwest Ghana, West Africa. This part of the continent lies on the northern flank of the Gulf of Guinea, in the equatorial zone of the Atlantic Ocean [6]. The "land nearest nowhere" refers to CTP, which is the land closest to a position in the sea that is at 0 latitude, 0 longitude, and 0 latitude [7]. Its approximately 570 km square area with water depths ranging from less than 10 meters (33 feet) to greater than 1500 meters (5000 feet), but most lies in water depths of less than 200 meters (700 feet). The basin has a thick portion of Upper Cretaceous drift, dominated by channel systems, stratigraphic traps, and basin floor fans. The Cretaceous Play is the functional play type, with Albian and Cenomanian-Turonian sandstones in tilted fault blocks serving as reservoirs and Turonian slope fan turbidite sandstones serving as source rocks [6]. The three wells under study in this basin are WELL_1X, WELL_2X and WELL_3X. WELL_1X was drilled to a total depth of 3792.322 m at a water depth of 109.1184 m. WELL_2X was also drilled to a total depth of 4892.04 m at a water depth of 2927 m. WELL_3X however was drilled to a total depth of 2587.904 m at a water depth of 780.8976 m.

## 3. Materials and Method

### 3.1. Materials

To evaluate and analyse the hydrocarbon potential in the Cape Three Points (CTP) reservoirs, the reservoir's petrophysical characteristics were estimated using the materials given below.

- Three (3) Wells (WELL_1X, WELL_2X and WELL_3X);
- Petrel Software;
- Techlog.

### 3.2. Methodology

The data was put into a format (.txt) acceptable by Petrel, a software provided by Schlumberger to help accurately estimate the set target for this study. The data was imported into Petrel and the appropriate ranges of the said parameters were set to convert the digitized well logging data into log curves (**Figure 1**) to help identify, analyse and estimate the petrophysical properties of the wells under study.

#### 3.2.1. Petrophysical Analysis of Log Values

It was required to read or choose log values in the various zones of interest as well as other crucial areas, including the shale or water-bearing zones, in order to conduct a log analysis. To turn the log into a series of distinct beds, specific log readings were selected from the vertical lines at the peaks and troughs and the horizontal lines drawn at each bed border at the inflection points on each curve.

#### 3.2.2. Evaluation of Petrophysical Properties of the Reservoirs

When assessing the CTP reservoirs' petrophysical characteristics, log curve signatures were generated in Petrel at different depths for the formation in the three wells (WELL_1X, WELL_2X and WELL_3X). The resulting information for each well generated was then exported from Petrel into Techlog to calculate the reservoir properties using the log calculator.

#### 3.2.3. Delineation of Hydrocarbon Bearing Zones

To delineate the reservoir and non-reservoir zones, API line with a value from the "curve" to the "level" for sandstone beds and from the "level" to the "curve" for the shale beds was specified. Thus, a value of 75 was chosen based on the comparison between the deep resistivity log and the gamma ray log which indicated sandstone from the curve at any value less than or equal to seventy-five

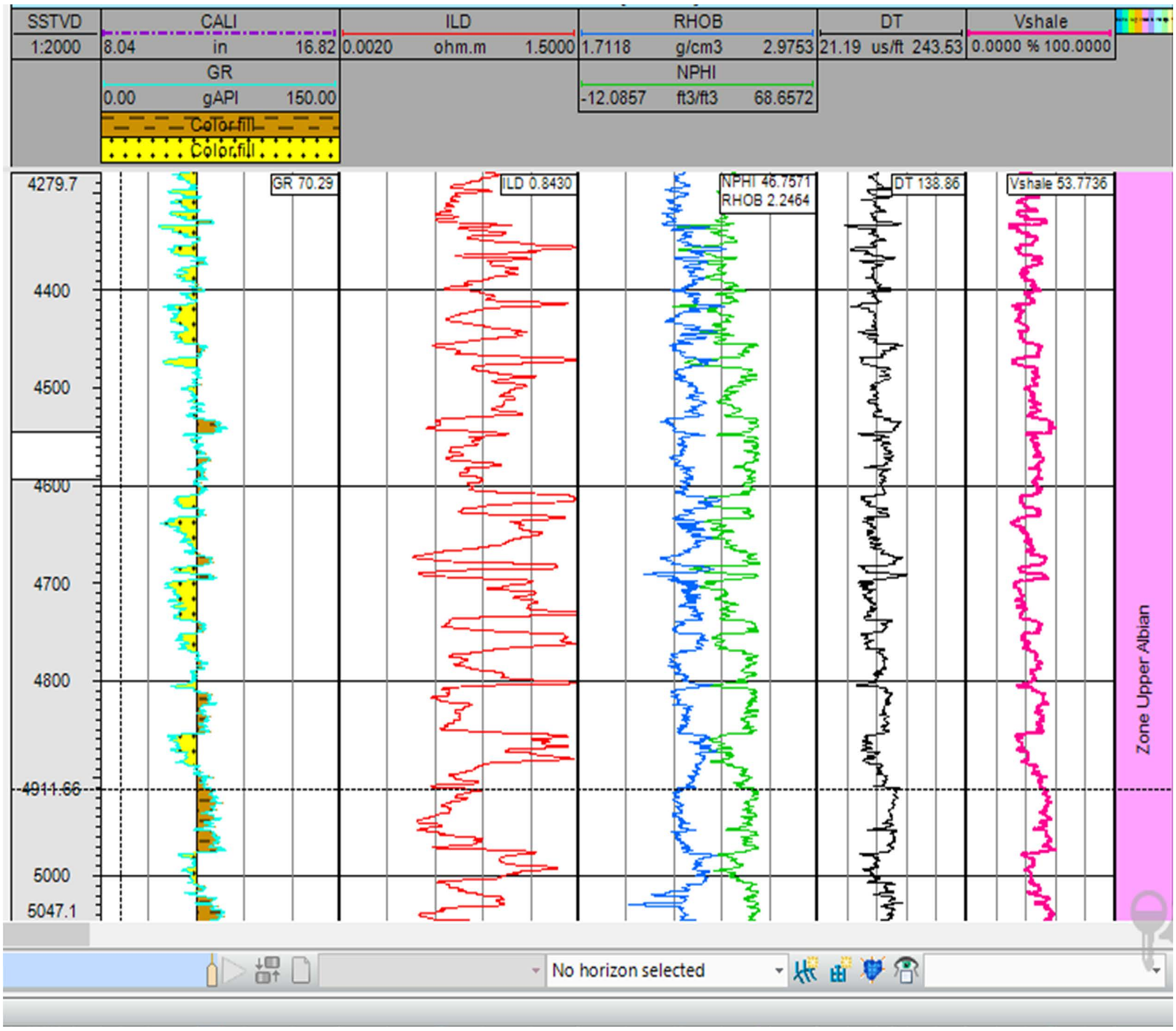


**Figure 1.** Log Curves for the WELL_1X in Petrel.

(75) and any value from the level or greater than seventy-five (75) to the curve on the right indicating shale beds. This was done to determine hydrocarbon bearing zones, reservoir thickness, net pay and net-gross ratio of the wells.

#### 3.2.4. Determination of the Thickness of the Gross Reservoir

The top and base of the reservoir sands were selected vertically across each well to determine the thickness of the gross reservoir. The thickness of the net reservoir was however determined by identifying the shale volume of the reservoir and subtracting it form the gross reservoir thickness.

#### 3.2.5. Shale Volume ($V_{sh}$) Estimation

The shale volume ($V_{sh}$) was determined linearly from the gamma ray logs by reading the values at both the shale line and clean sand line and substituting them as in Equation (1). This was done by drawing two vertical lines from the set API line (in this case 75). The first line was drawn to the maximum curve deviating to the left of the API line indicating clean sands whiles the other drawn to the maximum curve deviating to the right of the API line indicating the shale line.

$$V_{sh} = \frac{GR_{zone} - GR_{clean}}{GR_{shale} - GR_{clean}} \quad (1)$$

where:

$GR_{zone}$ is gamma ray log interest zone.

$GR_{clean}$ is sand bed in the gamma ray curve without any shale intercalations.

$GR_{shale}$ is 100% shale zone read from the gamma ray curve.

#### 3.2.6. Porosity Estimation

Equation (2) was utilized to determine the effective porosity of the interested zones using the density log.

$$\Phi_e = \left[\frac{\rho_{ma} - \rho_b}{\rho_{ma} - \rho_f}\right] - \left[\frac{\rho_{ma} - \rho_{sh}}{\rho_{ma} - \rho_f}\right] V_{sh} \quad (2)$$

where:

$\Phi_e$ is Density porosity (effective porosity).

$\rho_{ma}$ is matrix density ma.

$\rho_b$ is bulk density log reading.

$\rho_f$ is density of fluid.

$\rho_{sh}$ is density of shale.

$V_{sh}$ is shale volume.

#### 3.2.7. Permeability Estimation

The Wyllie and Rose (1950) empirical equation which proposes a relationship between Permeability, irreducible water saturation and porosity was used to estimate the permeability of the reservoirs since irreducible water saturation increases with internal surface area.

$$K = \frac{P\Phi^Q}{S_{wi}^R} \quad (3)$$

which is linearized if the equation is logarithmically transformed to.

$$\log K = \log P + Q \log \Phi - R \log S_{wi} \quad (4)$$

where $P$, $Q$ and $R$ are constants to be calibrated from core measurements.

#### 3.2.8. Estimation of Resistivity of Water

Resistivity of water, $R_w$ was calculated from the resistivity log curves in the sandstone strata with homogeneous intergranular porosity using Archie's water saturation equation.

$$(S_w)^n = \frac{aR_w}{\Phi^m R_t} \quad (5)$$

where,

$S_w$ is water saturation.

$R_t$ is formation Resistivity.

$\Phi$ is porosity.

Cementation factor = $n = m$.

Tortuosity factor ($a$) of 0.81 was used.

#### 3.2.9. Estimation of Estimation of Water Saturation

Even though Archie's formular is widely used to determine saturation of water, the Indonesian formular was used to determine the saturation of water for the reservoirs because it had shale intercalations which the Archie's equation doesn't consider.

$$\frac{1}{R_t}\left[\sqrt{\frac{\Phi_e^m}{aR_w}}+\frac{V_{sh}^{(1-0.5V_{sh})}}{\sqrt{R_{sh}}}\right]S_w^{0.5n} \tag{6}$$

where;

$R_t$ is formation (deep) resistivity.

$R_w$ is resistivity of water.

$\Phi_e$ is effective permeability.

$V_{sh}$ is shale volume.

$R_{sh}$ is shale resistivity.

$S_w$ is water saturation.

## 4. Results

Detailed results for each well were summarised in tabular form with cross plots of the various petrophysical properties presented in graphical form to ascertain whether or not the reservoirs are of good quality.

### 4.1. Reservoir Statistics

Table 1 presents the reservoir statistics findings for each of the three wells that were analysed using the previously described methods.

From Table 1, the gross reservoir thicknesses of the three wells (WELL_1X, WELL_2X and WELL_3X) are 812.58_m, 390.82_m and 62.94_m with their respective interval locations from 1203.06_m - 2015.64_m, 3863.03_m - 4253.85_m and 2497.38_m - 2560.32_m. WELL_1X has a net-gross ratio of 0.99, indicating that the WELL_1X reservoir contains 99% sandstone and 1% shale, whiles WELL_2X has a net-gross ratio of 0.96 indicating that the WELL_2X reservoir contains 96% sandstone and 4% shale and WELL_3X has a net-gross

Table 1. Reservoir statistics of each well.

| WELLS | Formation Top(m) | Formation Bottom (m) | Gross Reservoir Thickness (m) | Net Reservoir Thickness (m) | Net-Gross Ratio | No. of Sand Beds |
|---|---|---|---|---|---|---|
| WELL_1X | 1203.06 | 2015.64 | 812.58 | 803.54 | 0.99 | 18 |
| WELL_2X | 3863.03 | 4253.85 | 390.82 | 373.75 | 0.96 | 20 |
| WELL_3X | 2497.38 | 2560.32 | 62.94 | 23.76 | 0.38 | 20 |

ratio of 0.38 indicating that the WELL_3X reservoir contains 38% sandstone and 62% shale, shaly sands and calcite. The distribution of permeability, volume of shale, porosity and saturation of water in the reservoirs studied were determine using Techlog and discussed as follows.

### 4.2. Analysis of WELL_1X Reservoir Results

There were eighteen (18) sandstone beds in this reservoir with a net reservoir thickness of 803.54_m out of its gross thickness of 812.58_m. Generally, it can be inferred from **Table 2** and **Figure 2** that porosity decreased with permeability except for zones 1, 4, 14 and 18 which had very high permeability. This could be because the reservoir rock may be fractured in those zones. With an average porosity value of 0.13, this reservoir rock may be classified as fairly porous (Aseidu, 2014) due to poor grain packing which is evident in **Figure 3**, a cross plot of gamma ray against bulk density showing how densely the grains were packed reducing the effective porosity and permeability of the WELL_1X reservoir. The average water saturation value of 0.94 obtained from the sandstone zones of this reservoir rock suggested the reservoir contained 94% water and 6% hydrocarbon. This is evident in both **Figure 4** and **Figure 5**. A cross plot of deep resistivity

**Table 2.** Summary results obtained from the WELL_1X Reservoir.

| Zone | Depth (m) | Reservoir Thickness (m) | K (md) | PHIE_D | SWE_INDO | VSH_GR |
|---|---|---|---|---|---|---|
| 1 | 1203.06 - 1382.55 | 179.49 | 1299.19 | 0.17 | 0.87 | 0.40 |
| 2 | 1382.73 - 1383.79 | 1.06 | 579.49 | 0.17 | 0.80 | 0.56 |
| 3 | 1384.39 - 1384.86 | 0.47 | 444.15 | 0.15 | 0.79 | 0.57 |
| 4 | 1385.32 - 1501.12 | 115.80 | 353.09 | 0.14 | 0.94 | 0.53 |
| 5 | 1501.44 - 1506.16 | 4.72 | 63.23 | 0.10 | 1.00 | 0.47 |
| 6 | 1506.31 - 1515.17 | 8.86 | 186.25 | 0.12 | 0.98 | 0.61 |
| 7 | 1515.32 - 1515.75 | 0.44 | 354.58 | 0.15 | 1.00 | 0.69 |
| 8 | 1516.22 - 1534.81 | 18.60 | 259.91 | 0.13 | 0.98 | 0.65 |
| 9 | 1536.04 - 1536.51 | 0.47 | 71.33 | 0.10 | 1.00 | 0.54 |
| 10 | 1536.94 - 1542.89 | 5.95 | 66.04 | 0.10 | 0.98 | 0.51 |
| 11 | 1543.35 - 1545.63 | 2.27 | 689.66 | 0.16 | 0.91 | 0.57 |
| 12 | 1546.38 - 1547.32 | 0.93 | 864.83 | 0.16 | 0.84 | 0.62 |
| 13 | 1547.46 - 1550.67 | 3.21 | 1596.55 | 0.17 | 0.84 | 0.66 |
| 14 | 1550.82 - 1589.07 | 36.87 | 459.96 | 0.13 | 0.97 | 0.64 |
| 15 | 1589.23 - 1596.37 | 7.14 | 117.96 | 0.10 | 0.98 | 0.61 |
| 16 | 1596.55 - 1597.92 | 1.37 | 43.32 | 0.08 | 0.99 | 0.62 |
| 17 | 1598.53 - 1598.68 | 0.14 | 4.04 | 0.05 | 1.00 | 0.62 |
| 18 | 1599.43 - 2015.18 | 415.74 | 273.71 | 0.11 | 0.97 | 0.52 |

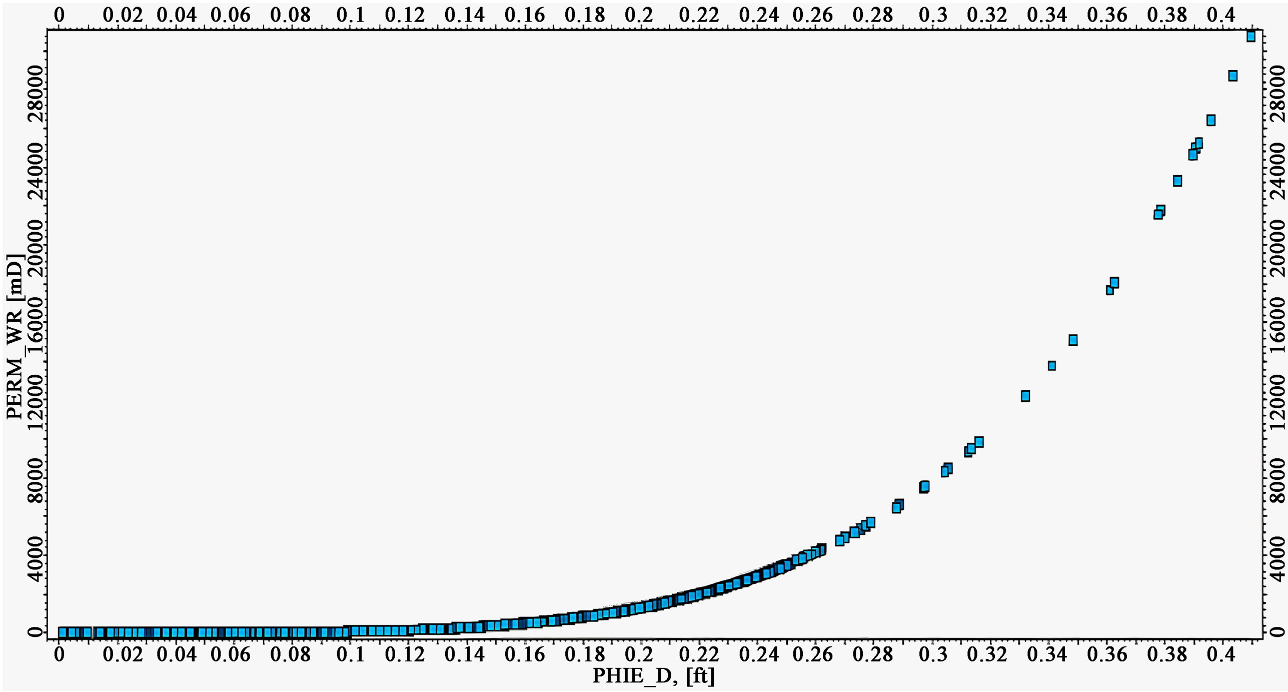


**Figure 2.** Permeability verse effective porosity cross plot for WELL_1X.

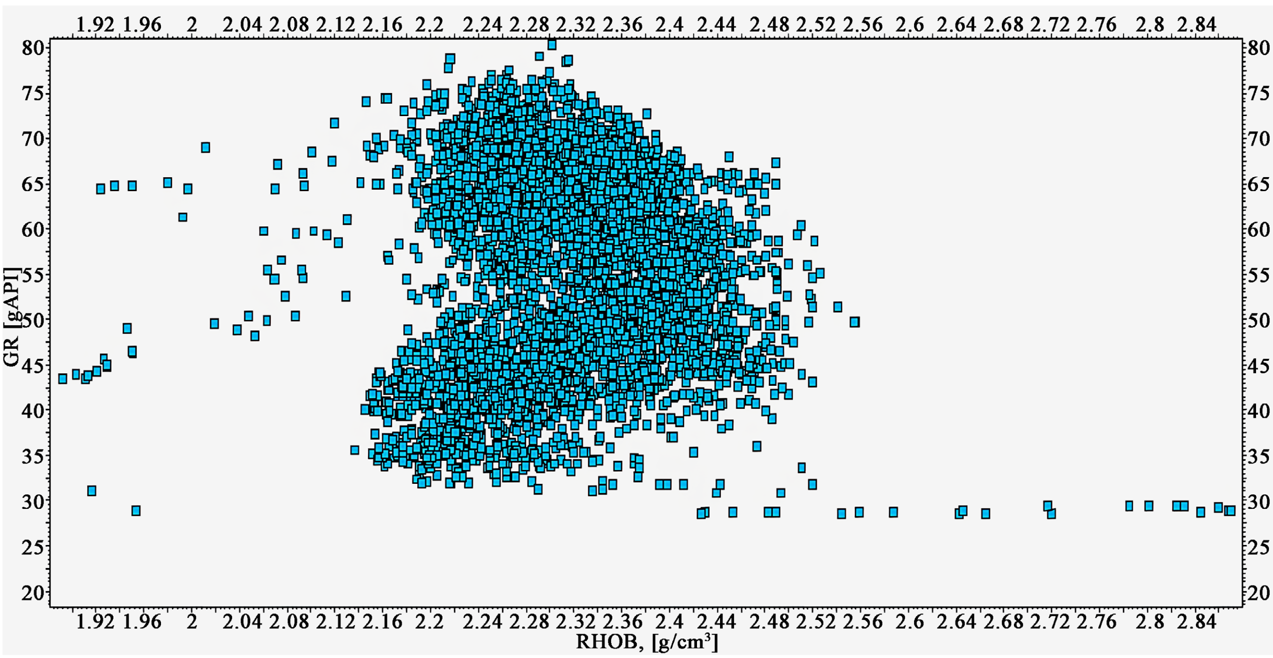


**Figure 3.** Gamma ray verse bulk density cross plot for WELL_1X.

verse water saturation in **Figure 4** verified the very low or no hydrocarbon content in this reservoir whiles **Figure 5**, a cross plot of Gamma Ray against deep resistivity verified the general low readings of the resistivity log in **Figure 6**, due to low hydrocarbon content. From all the results obtained from the petrophysical evaluation of the WELL_1X reservoir, one could say that this reservoir is of bad quality.

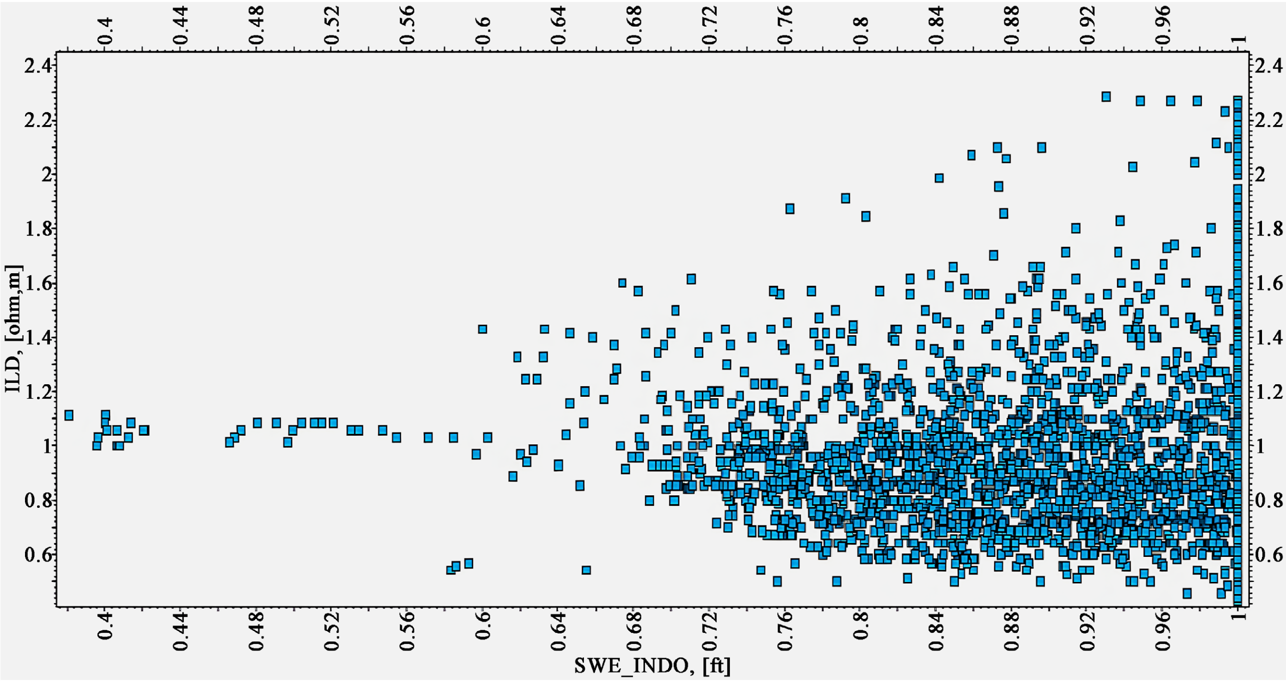


**Figure 4.** Deep resistivity verse water saturation cross plot for WELL_1X.

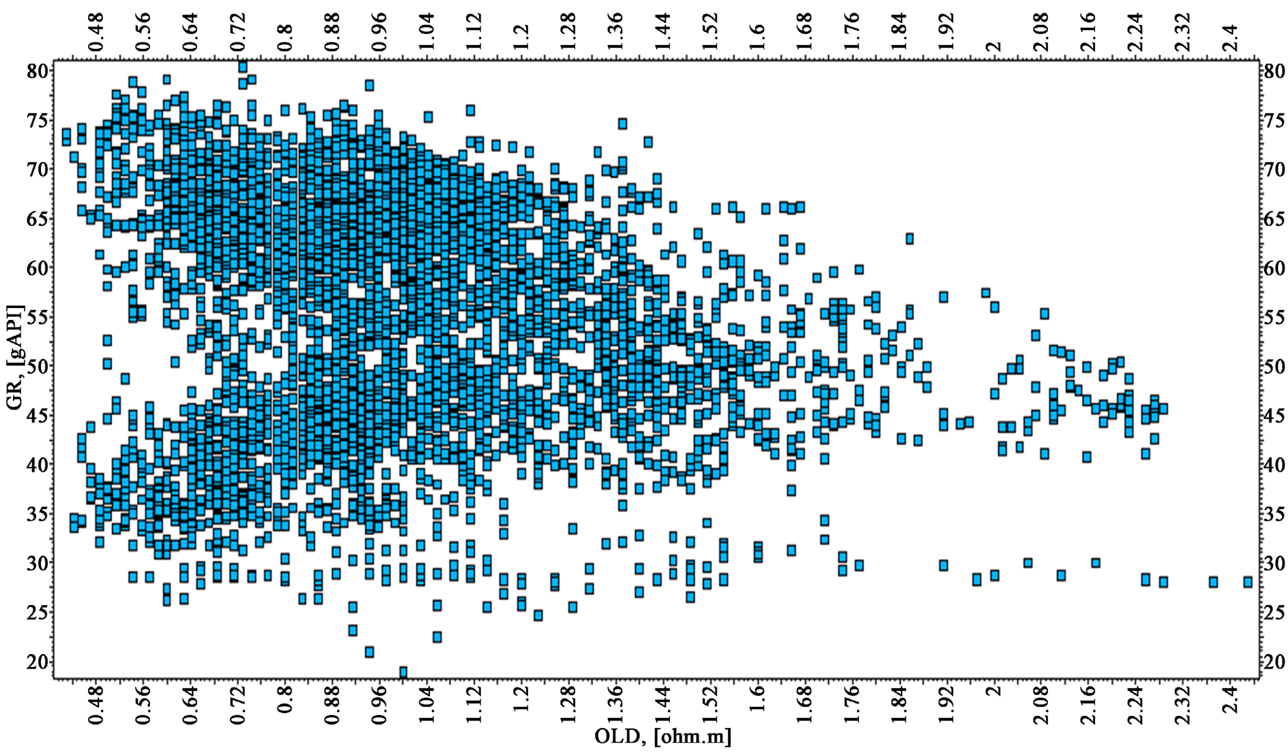


**Figure 5.** Gamma ray verse deep resistivity cross plot for WELL_1X.

### 4.3. Analysis of WELL_2X Reservoir Results

There were twenty (20) sandstone zones in this reservoir with a net reservoir thickness of 373.75_m out of a gross thickness of 390.82_m. Generally, it could be inferred from **Table 3** and **Figure 7** that porosity and permeability values

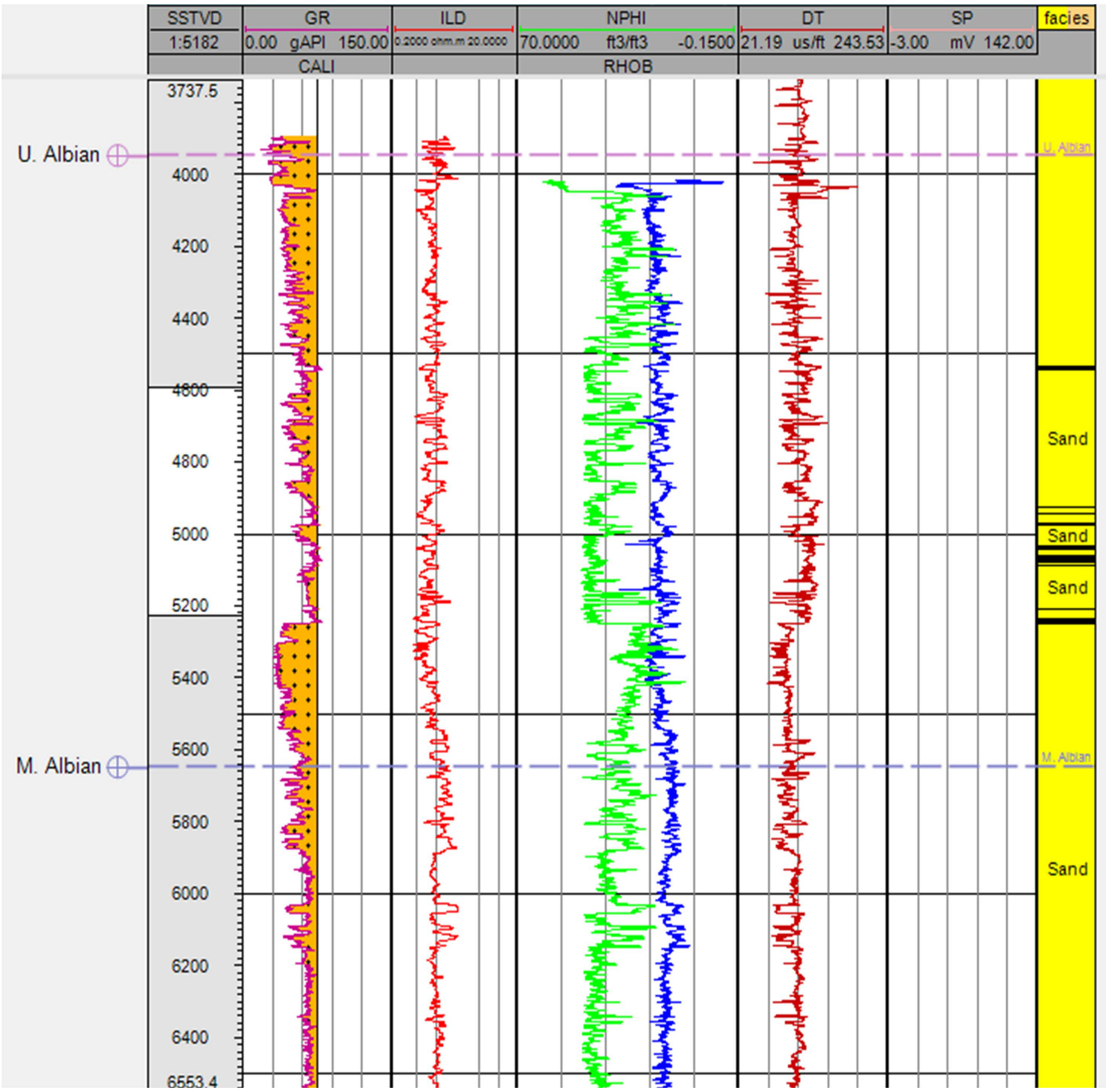


**Figure 6.** Well log section display of WELL_1X.

obtained were very low with the exception of zones 1 and 2 which had very high permeability. This could also be because the reservoir rock may be fractured in these zones. With an average porosity value of 0.03, this reservoir rock may be classified to have insignificant porosity due to depositional and post depositional processes such as compaction, cementation and recrystallization (Ali *et al.* 2010) which is evident in Figure 8, a cross plot of gamma ray against bulk density showing how densely the grains were packed reducing the effective porosity and permeability of the WELL_2X reservoir. The average water saturation value of 0.95 obtained from the sandstone zones of this reservoir rock suggested the reservoir contains 95% water and 5% hydrocarbon. This was evident in both Figure 9 and Figure 10. A cross plot of deep resistivity verse water saturation in Figure 9 verified the very low or no hydrocarbon content in this reservoir whiles

**Table 3.** Summary results obtained from the WELL_2X Reservoir.

| Zone | Depth (m) | Reservoir Thickness (m) | K (md) | PHIE_D | SWE_INDO | VSH_GR |
|---|---|---|---|---|---|---|
| 1 | 3863.03 - 3892.29 | 29.26 | 22,012.24 | 0.03 | 0.88 | 0.42 |
| 2 | 3892.92 - 3899.01 | 6.09 | 1,171,875 | 0.41 | 0.62 | 0.35 |
| 3 | 3899.33 - 3926.14 | 26.81 | 0.16 | 0.004 | 0.99 | 0.52 |
| 4 | 3926.45 - 3932.23 | 5.77 | 0.70 | 0.02 | 0.96 | 0.52 |
| 5 | 3934.05 - 3977.94 | 43.89 | 6.00 | 0.03 | 0.90 | 0.51 |
| 6 | 3978.57 - 3986.79 | 8.22 | 3.88 | 0.007 | 0.97 | 0.56 |
| 7 | 3988.61 - 4055.12 | 66.51 | 4.99 | 0.04 | 0.87 | 0.41 |
| 8 | 4055.67 - 4094.98 | 39.30 | 5.65 | 0.04 | 0.87 | 0.42 |
| 9 | 4095.61 - 4102.96 | 7.35 | 0.001 | 0.001 | 1.00 | 0.60 |
| 10 | 4103.52 - 4165.14 | 61.62 | 3.84 | 0.02 | 0.93 | 0.44 |
| 11 | 4166.94 - 4173.66 | 6.72 | 1.51 | 0.01 | 0.98 | 0.52 |
| 12 | 4175.17 - 4185.84 | 10.67 | 1.34 | 0.00 | 0.99 | 0.54 |
| 13 | 4186.79 - 4193.75 | 6.72 | 0.00 | 0.00 | 1.00 | 0.62 |
| 14 | 4194.70 - 4195.88 | 1.19 | 0.00 | 0.00 | 1.00 | 0.49 |
| 15 | 4196.52 - 4208.70 | 12.18 | 0.00 | 0.00 | 1.00 | 0.64 |
| 16 | 4209.01 - 4216.29 | 7.28 | 0.85 | 0.01 | 0.97 | 0.49 |
| 17 | 4216.92 - 4219.05 | 2.13 | 0.20 | 0.01 | 1.00 | 0.50 |
| 18 | 4219.69 - 4228.55 | 8.86 | 0.18 | 0.002 | 1.00 | 0.57 |
| 19 | 4228.86 - 4240.09 | 11.23 | 1.39 | 0.01 | 0.98 | 0.51 |
| 20 | 4241.59 - 4253.54 | 11.94 | 0.25 | 0.01 | 1.00 | 0.54 |

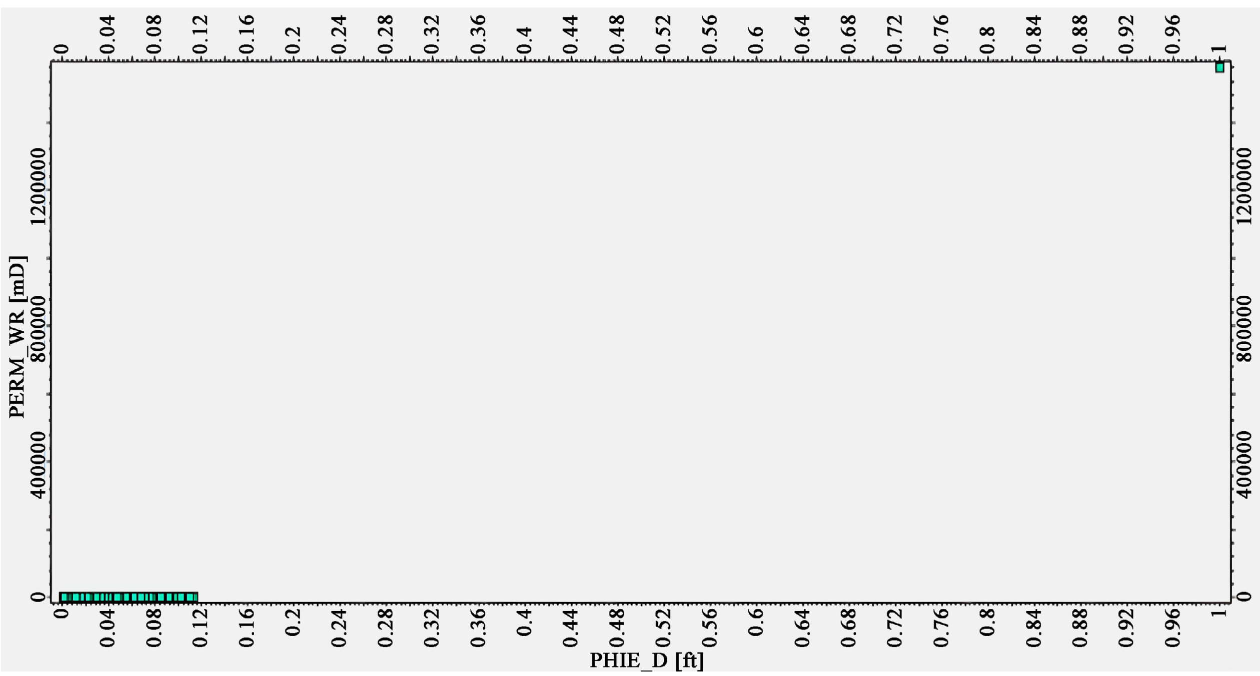


**Figure 7.** Permeability Verse Effective Porosity Cross Plot for WELL_2X.

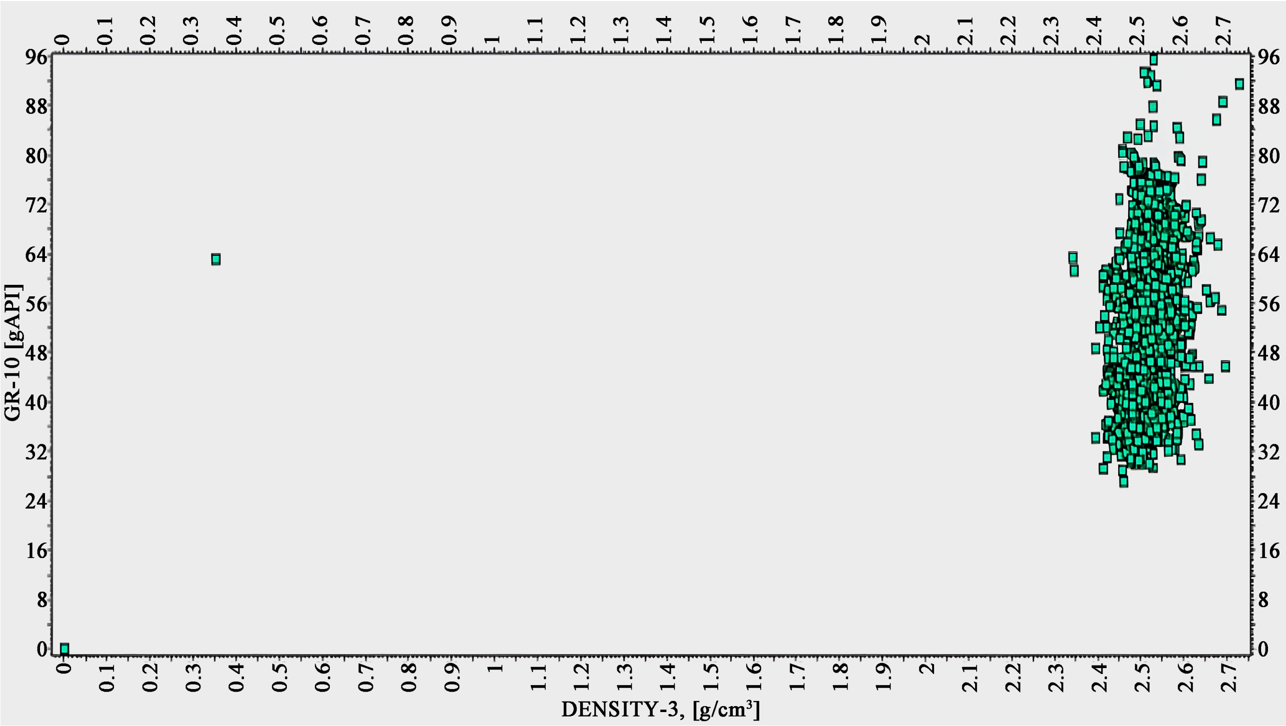


**Figure 8.** Gamma ray verse bulk density cross plot for WELL_2X.

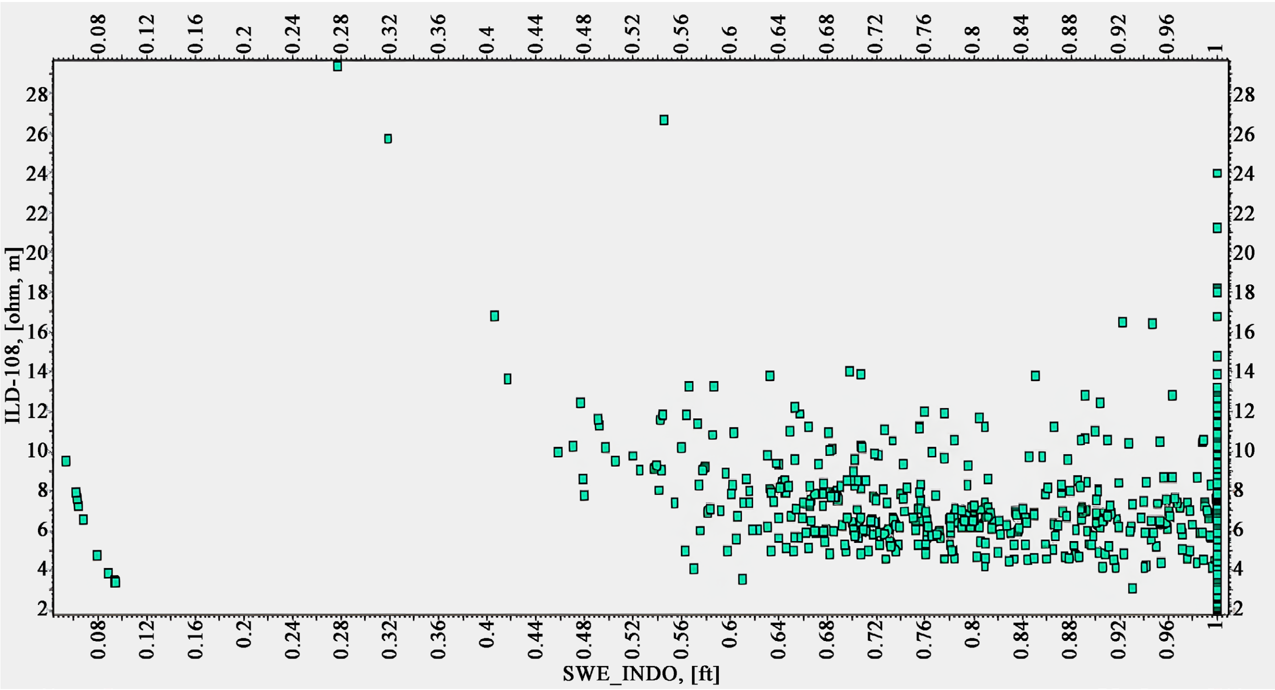


**Figure 9.** Deep resistivity verse water saturation cross plot for WELL_2X.

**Figure 10**, a cross plot of Gamma Ray against deep resistivity verified the general low readings of the resistivity log in **Figure 11**, due to low hydrocarbon content. From all the results obtained from the petrophysical evaluation of the WELL_2X reservoir, one could say that this reservoir is of bad quality.

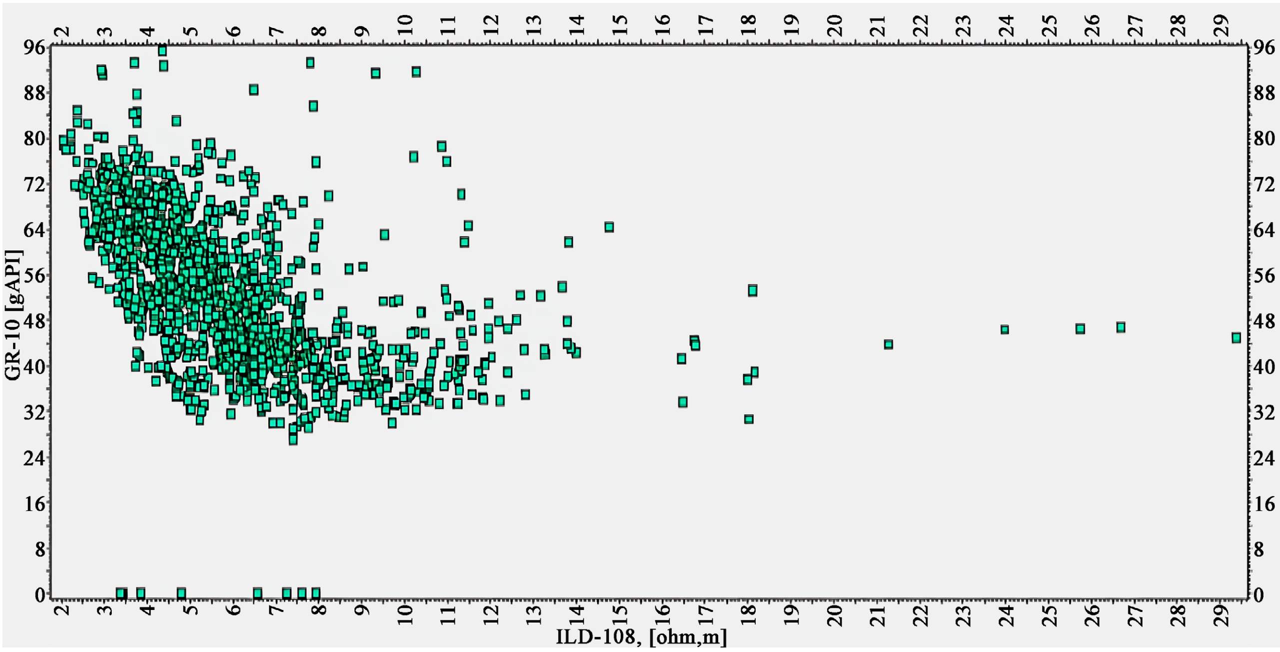


**Figure 10.** Gamma ray verse deep resistivity cross plot for WELL_2X.

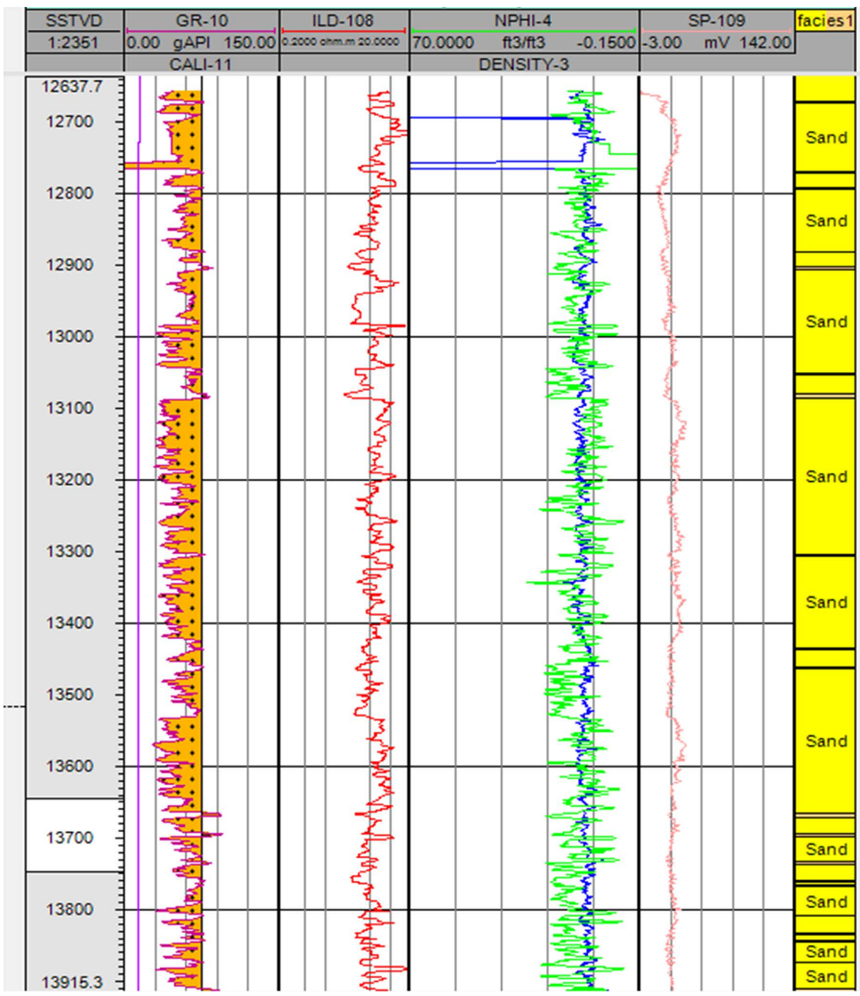


**Figure 11.** Well log section display of WELL_2X.

### 4.4. Analysis of WELL_3X Reservoir Results

There were twenty (20) sandstone zones in this reservoir with a net reservoir thickness of 23.76_m out of its gross thickness of 62.94_m. Generally, it could be inferred from Table 4 and Figure 12 that the permeability in all the sandstone zones of this reservoir was very high as compared to the low values obtained for porosity. This could be because the reservoir rock may be fractured. With an average porosity value of 0.11, this reservoir rock may be classified as fairly porous (Aseidu, 2014) which is evident in Figure 13, a cross plot of gamma ray against bulk density showing a less dense distribution. This could be due to large pore throat between sandstone grains of the WELL_3X reservoir. The average water saturation value of 0.89 obtained from the sandstone zones of this reservoir rock suggested that the reservoir contained 89% water and 11% hydrocarbon. This is evident in both Figure 14 and Figure 15. A cross plot of deep resistivity verse water saturation in Figure 14 verified the low hydrocarbon content in this

**Table 4.** Summary results obtained from the WELL_3X Reservoir.

| Zone | Depth (m) | Reservoir Thickness (m) | K (md) | PHIE_D | SWE_INDO | VSH_GR |
|---|---|---|---|---|---|---|
| 1 | 2497.38 - 2500.89 | 3.51 | 132.26 | 0.11 | 0.82 | 0.67 |
| 2 | 2501.05 - 2504.24 | 3.19 | 59.13 | 0.09 | 0.98 | 0.58 |
| 3 | 2504.40 - 2504.56 | 0.16 | 57.48 | 0.10 | 1.00 | 0.61 |
| 4 | 2505.01 - 2506.38 | 1.37 | 119.60 | 0.11 | 0.89 | 0.65 |
| 5 | 2507.90 - 2508.04 | 0.14 | 60.29 | 0.10 | 0.98 | 0.69 |
| 6 | 2508.20 - 2514.46 | 6.26 | 92.81 | 0.10 | 0.90 | 0.63 |
| 7 | 2514.60 - 2515.22 | 0.62 | 391.10 | 0.15 | 0.68 | 0.56 |
| 8 | 2515.51 - 2517.97 | 2.46 | 202.64 | 0.13 | 0.72 | 0.70 |
| 9 | 2522.39 - 2522.52 | 0.14 | 25.45 | 0.09 | 1.00 | 0.80 |
| 10 | 2522.84 - 2522.98 | 0.14 | 113.42 | 0.11 | 0.91 | 0.76 |
| 11 | 2523.30 - 2524.05 | 0.75 | 57.63 | 0.10 | 0.96 | 0.77 |
| 12 | 2524.37 - 2525.58 | 1.21 | 75.00 | 0.10 | 0.96 | 0.65 |
| 13 | 2525.73 - 2526.03 | 0.30 | 146.63 | 0.12 | 0.89 | 0.52 |
| 14 | 2526.19 - 2526.94 | 0.75 | 168.16 | 0.13 | 0.90 | 0.57 |
| 15 | 2527.10 - 2528.17 | 1.07 | 101.36 | 0.11 | 0.93 | 0.65 |
| 16 | 2528.33 - 2528.47 | 0.14 | 67.85 | 0.11 | 0.96 | 0.70 |
| 17 | 2531.36 - 2531.70 | 0.34 | 218.99 | 0.13 | 0.83 | 0.63 |
| 18 | 2535.03 - 2535.19 | 0.16 | 97.88 | 0.11 | 0.86 | 0.80 |
| 19 | 2535.64 - 2536.55 | 0.91 | 238.54 | 0.13 | 0.76 | 0.61 |
| 20 | 2537.01 - 2537.17 | 0.16 | 193.55 | 0.13 | 0.82 | 0.57 |

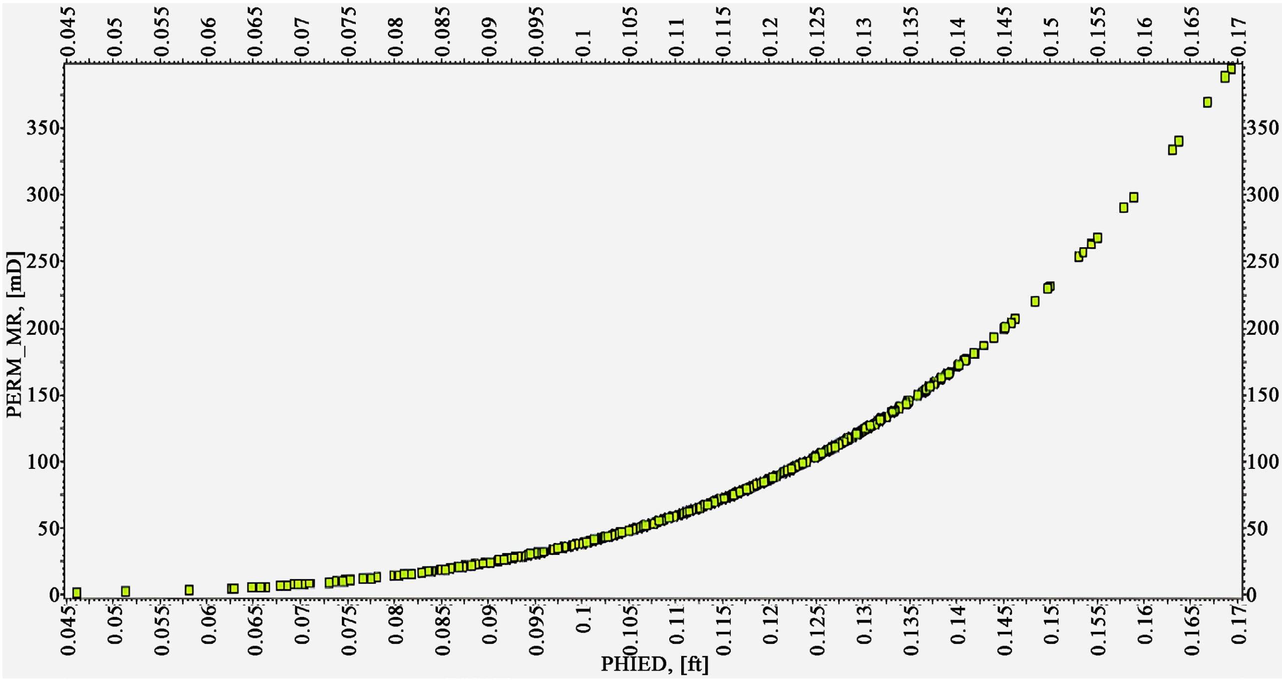


**Figure 12.** Permeability verse effective porosity cross plot for WELL_3X.

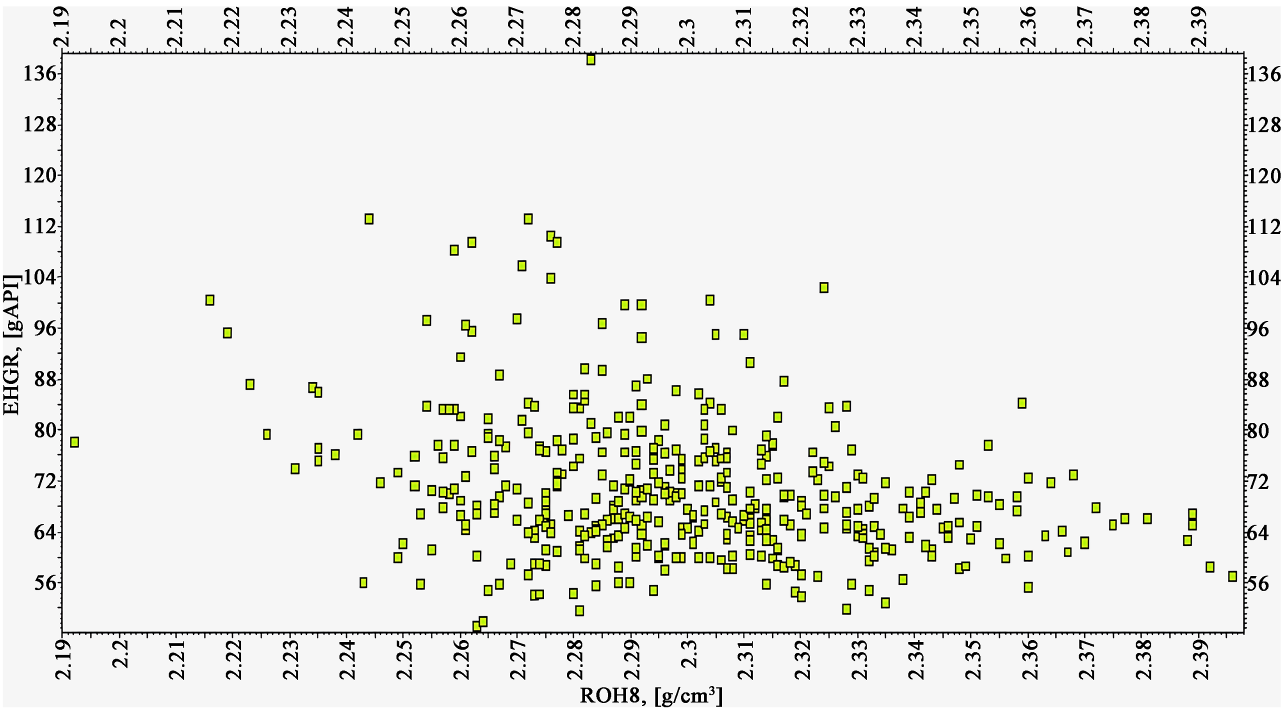


**Figure 13.** Gamma ray verse bulk density cross plot for WELL_3X.

reservoir whiles **Figure 13**, a cross plot of Gamma Ray against deep resistivity verified the general average readings of the resistivity log in **Figure 16**, due to low hydrocarbon content. From all the results obtained from the petrophysical evaluation of the WELL_3X reservoir, showed that the reservoir is of better quality than the previous two reservoirs.

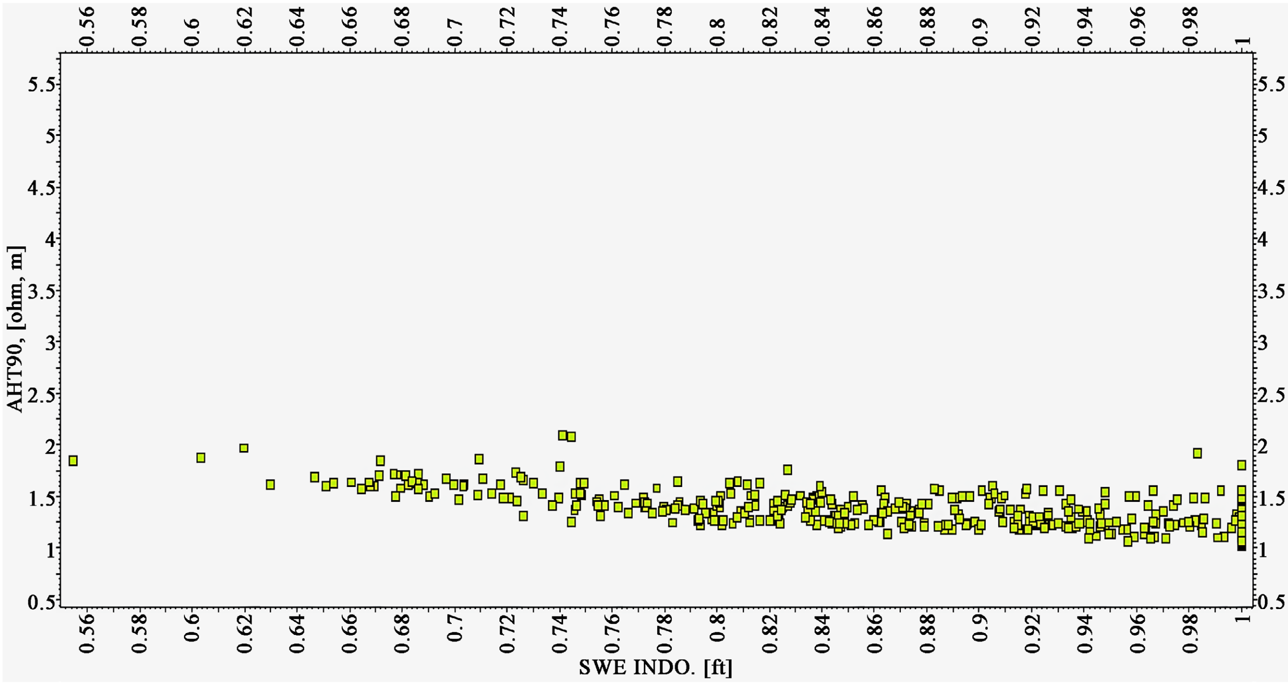


**Figure 14.** Deep resistivity verse water saturation cross plot for WELL_3X.

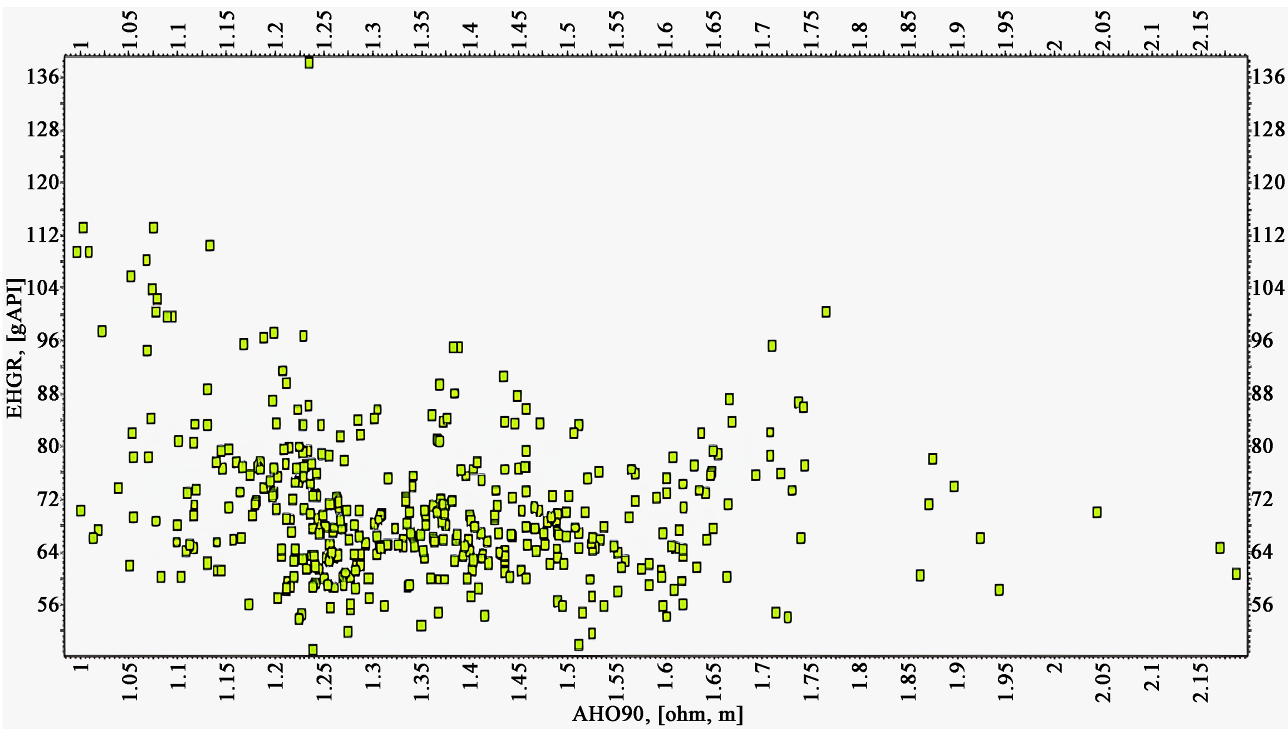


**Figure 15.** Gamma ray verse deep resistivity cross plot for WELL_3X.

## 5. Conclusions

Formation evaluation methods were applied successfully to wireline log data from three exploratory wells in the Cape Three Points basin. Composite well logs of the three exploratory wells studied revealed two major lithological units;

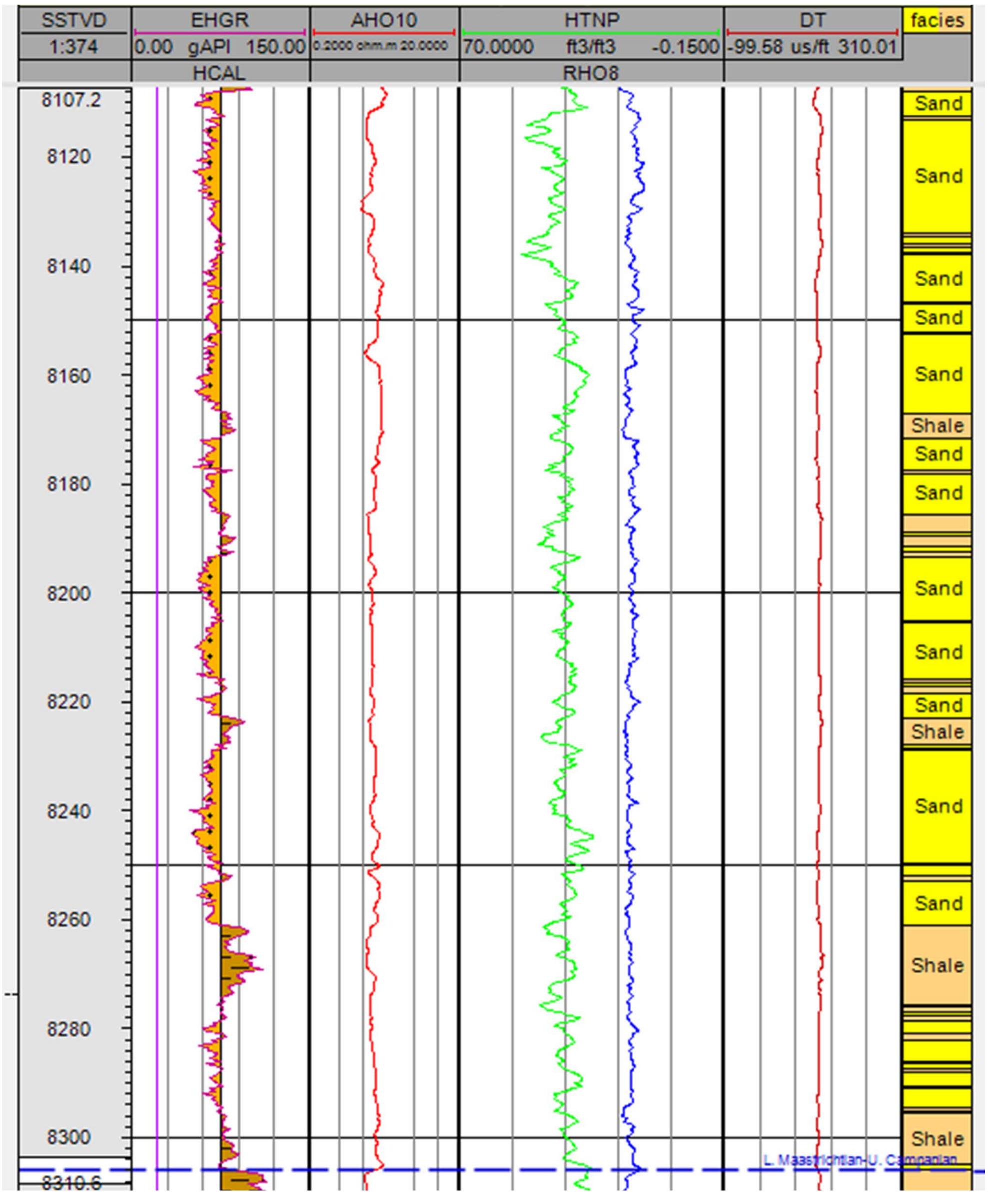


**Figure 16.** Well log section display of WELL_3X

sandstone and shale, for all the reservoir formations studied. The petrophysical evaluation of the three wells, WELL_1X, WELL_2X and WELL_3X at Tano Cape Three Points basin was made possible by the analysis of well log responses from these wells. The results obtained from the analysis of the petrophysical properties; permeability, volume of shale, porosity, water saturation and reservoir thickness were used in estimating the possibilities of the reservoirs containing hydrocarbon. The resulting distribution of these estimated parameters from the well log calculations gave average porosities of 13%, 3% and 11% respectively with very high values of permeability due to fracturing. And the average water saturation values of 94%, 95% and 89% for the wells; WELL_1X, WELL_2X and WELL_3X allowed the following conclusions to be drawn.

1) All the reservoirs studied were fairly porous and cannot be good hydrocar-

bon bearing zones.

2) All the exploratory wells used in this research are wildcat wells because of their water saturation values.

## Acknowledgements

For providing the materials and resources for this paper, the authors would like to thank Schlumberger and the Ghana National Petroleum Corporation (GNPC).

## Conflicts of Interest

The authors declare no conflicts of interest regarding the publication of this paper.

## References

[1] Glover, P.W.J. (2000) Petrophysics. Master's Thesis, University of Aberdeen, Aberdeen. https://pdfcoffee.com/paul-glover-petrophysics-pdf-free.html

[2] Macini, P. and Mesini, E. Petrophysics and Reservoir Characteristics. https://www.eolss.net/sample-chapters/C08/E6-193-05.pdf

[3] Ahr, W.M. (2011) Geology of Carbonate Reservoirs: The Identification, Description and Characterization of Hydrocarbon Reservoirs in Carbonate Rocks. John Wiley & Sons, New York.

[4] Worthington, P. (2011) The Petrophysics of Problematic Reservoirs. Journal of Petroleum Technology, **63**, 88-97. https://doi.org/10.2118/144688-JPT

[5] Darling, T. (2005) Well Logging and Formation Evaluation. Elsevier.

[6] Adda, G.W. (2013) The Petroleum Geology and Prospectivity of the Neo-Proterozoic, Paleozoic and Cretaceous Sedimentary Basins in Ghana. AAPG.

[7] Wikipedia (2014) Cape Three Points. https://en.wikipedia.org/wiki/Cape_Three_Points